



## BARKHAUSEN NOISE AS A MAGNETIC NONDESTRUCTIVE TESTING TECHNIQUE

Ömer ADANUR<sup>1</sup>, Oğuz KOÇAR<sup>2</sup>, Ahmet Serdar GÜLDİBİ<sup>3\*</sup>, Engin KOCAMAN<sup>4</sup>, Erhan BAYSAL<sup>5</sup>

<sup>1</sup>Sakarya University of Applied Sciences, Faculty of Engineering, Department of Manufacturing Engineering, 54100, Sakarya, Türkiye

<sup>2</sup>Zonguldak Bülent Ecevit University, Faculty of Engineering, Department of Mechanical Engineering, 67980, Zonguldak, Türkiye

<sup>3</sup>Karabük University, Faculty of Technology, Department of Manufacturing Engineering, 78000, Karabük, Türkiye

<sup>4</sup>Zonguldak Bülent Ecevit University, Faculty of Engineering, Department of Aerospace Engineering, 67980, Zonguldak, Türkiye


<sup>5</sup>Zonguldak Bülent Ecevit University, Alaplı Vocational School, 67980, Zonguldak, Türkiye


**Abstract:** Magnetic Barkhausen Noise (MBN) is a magnetic-based non-destructive electromagnetic testing method. Due to the electromagnetic working principle of MBN, it can be used for ferromagnetic materials, which consist of small magnetic fields discredited by domain walls and oriented in various directions. In an external magnetic field application, the fields turn to the magnetic direction, and the domain walls move and cause magnetic flux jumps. The jumps are named Barkhausen Noise (BN). The domain wall movements are sometimes pushed down by microstructure, composition, and defects. As the magnetic domain walls break away from the pinning sites produce MBN signal. MBN can be used for different material properties such as microstructure, composition, residual stress, and hardness. The paper's purpose is to analyze MBN as an improved NDT, clarify the relationship between material properties and MBN profile, and introduce MBN's applications and test equipment of MBN.


**Keywords:** Magnetic barkhausen noise, Material properties, MBN applications, MBN experimental setup, MBN signal, Non-Destructive testing


\*Corresponding author: Karabük University, Faculty of Technology, Department of Manufacturing Engineering, 78000, Karabük, Türkiye


E mail: serdarguldibi@karabuk.edu.tr (A.S. GÜLDİBİ)

Ömer ADANUR  <https://orcid.org/0000-0001-5591-9661>

Oğuz KOÇAR  <https://orcid.org/0000-0002-1928-4301>

Ahmet Serdar GÜLDİBİ  <https://orcid.org/0000-0001-7021-060X>

Engin KOCAMAN  <https://orcid.org/0000-0001-5617-3064>

Erhan BAYSAL  <https://orcid.org/0000-0002-2767-8722>

Received: December 01, 2023

Accepted: May 15, 2024

Published: July 15, 2024

**Cite as:** Adanur Ö, Koçar O, Güldibi AS, Kocaman E, Baysal E. 2024. Barkhausen noise as a magnetic nondestructive testing technique. *BSJ Eng Sci*, 7(4): 785-796.

### 1. Introduction

Materials and manufactured/products often need to be tested before distribution to ensure they meet expectations and ensure quality during a specified period of service (Blitz, 2012). The industry has two kinds of test methods: destructive test methods (DT) and non-destructive test methods (NDT).

In destructive testing, tests usually contain the deformation or failure of samples/material (called test samples or pieces) to determine mechanical properties, such as strength, toughness, and hardness. DT can be used to predict the performance of products during their service life. However, for the predictions to be reliable, the test conditions must be very similar to the environment in which the product operates. However, there are certain limitations in the test conditions and, therefore, cannot be applied to the products in service (McMaster, 1959). In NDT, these tests are performed without any damage to the product. Thus, the product can continue to be used. Hence, it is called "non-destructive testing". NDTs can be used for semi-products, materials, assemblies, or constructions. NDTs are often required to verify the quality and estimate a product's or

system's strength and serviceability. There are many NDT methods. Each of these is based on various physical features. NDT methods can be listed as visual, penetrant, pressure and leak, acoustic, thermal, radiography, magnetic, electrical and electrostatic, and electromagnetic induction (Ping et al., 2010). One of the non-destructive methods is MBN measurement, which is advisable for ferromagnetic materials and is an electromagnetic testing method (Cullity and Graham, 2011) used mainly in the aviation and automotive industry. The method of BN has been quite common due to its compliance with automation, being fast, and enabling characterization with the measurement of parameters (Yelbay, 2008). In 1907, the domain theory of ferromagnetism was first introduced by the French physicist Pierre-Ernest Weiss (Fischer, 2013). In 1919, Barkhausen found "noise" in an earphone during a piece of iron-induced voltage in a pick-up coil. He found the sound of magnetization changes during induction and was called "Magnetic Barkhausen Noise." This experiment is the first evidence of the presence of magnetic domains in a ferromagnetic material (Clapham et al., 2000). A ferromagnetic material is comprised of



magnetic domains (magnetic areas in microscopic dimensions). Magnetic domains are separated from each other by domain walls. Magnetization in domain limits is dispersed in a homogenized way, and there are 1012-1018 dipoles oriented in the same direction in magnetic domains (Yelbay, 2008). Though the domains are oriented the same within themselves, they are oriented randomly according to other domains. Thus, the average effect of magnetism is set to zero, and metal does not have any specific magnetic characteristics (Cullity and Graham, 2011). When an external magnetic field is applied to the material, domain walls start to move. When the magnitude of the applied magnetic field reaches a sufficient level, domains create a single field, moving the domain walls away (Figure 1), and dipoles are oriented in the same direction. Thus, the metal will have a powerful magnetism (Lo et al., 2000; Durin and Zapperi, 2004).

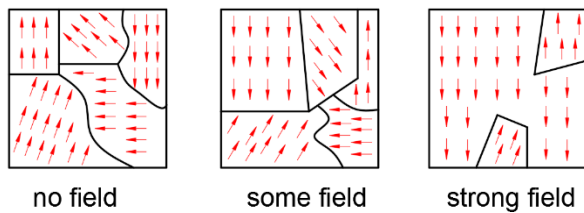


Figure 1. Movement of domain walls.

Even if the magnetic field changes correctly during the movements of the domain walls, jumps occur over the hysteresis curve. These abrupt jumps cause rapid changes in the magnetization of the material. Due to these changes, a signal like a noise called MBN arises. This signal gives information on many characteristics of the material, such as its particle size (Yelbay, 2008), residual stress (Cullity and Graham, 2011), or phase ratios.

This article introduces the necessary equipment for MBN measurements giving explanations of basic concepts of MBN. Moreover, its areas of usage and the relation of the BN signal with the characteristics of the material are clarified.

## 2. Magnetic Barkhausen Noise Methods

### 2.1. Basis of MBN

When ferromagnetic materials are exposed to an external magnetic field, atoms comprising the material line up with their poles in the same direction. This causes the material to demonstrate the characteristics of the magnet. With these materials, the relation between magnetic field strength "H" and magnetization "M" is not linear. The material forms following the first magnetization curve during "M" (magnetization). This curve has a high slope at first, but later, as the material gets closer to the point of magnetic saturation, the slope of the curve declines. After the material reaches saturation, even if we raise the strength of the magnetic field, the material cannot be magnetized anymore. After

this point, if the magnetic field's strength is reduced, the time curve starts to follow a different path. When the magnetic field strength is reduced to zero, magnetization is still on the material called "retentivity" (remanence). When the relation of H-M is observed on magnetic fields that act in two opposite directions, the hysteresis curve appears (Figure 2) (Graham and Chikazumi, 1997). If the hysteresis loops of ferromagnetic material are analyzed in high resolution, discontinuous magnetic flux bounces are observed (Figure 3). The reason is that the domain walls' movements are shaky and discontinuous (Paper et al., 2000).

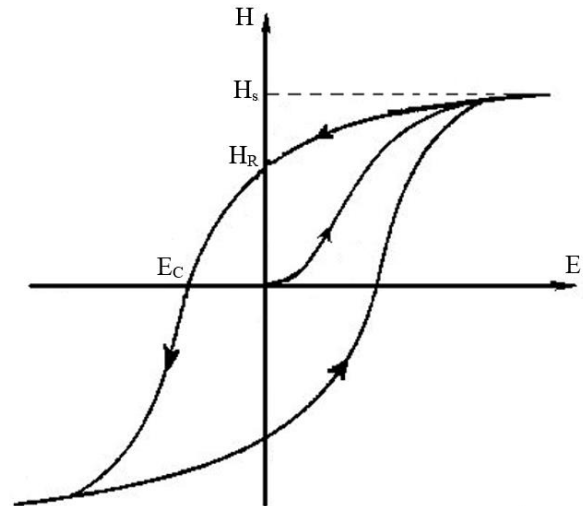


Figure 2. Hysteresis loop (Graham and Chikazumi, 1997).

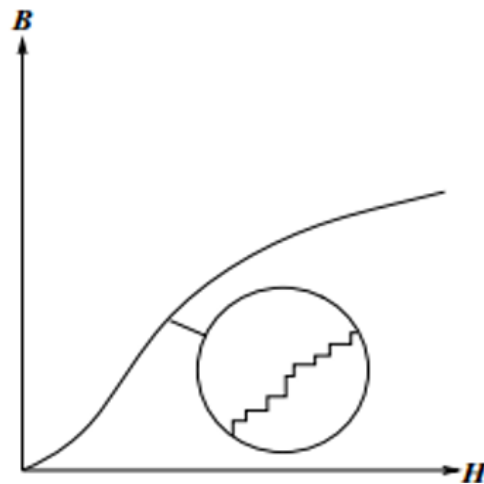


Figure 3. Magnetic flux jumps on hysteresis.

As a result of an applied magnetic field, domain walls start to move. Domain walls run through defects in the internal structure during their movements. The internal structure of the metals is not perfect and consists of defects. These defects can be dislocations, residual micro stresses, and particle boundaries (Kemal and Gür, 2008). These parts in the material's internal structure are called "pinning sites." Domain walls squeeze between these fields, and when the external magnetic field is powerful

enough, they suddenly split away from their coupling points in an irreversible way (Figure 4). Sudden bounces that occurred during the split cause abrupt changes in magnetic flux. With the determination of these changes, a signal like a noise comes out called BN noise. It is the effect of crystal structure defects just as the dislocations on magnetization (Graham and Chikazumi, 1997; Spaldin, 2010; Manh et al. 2020).

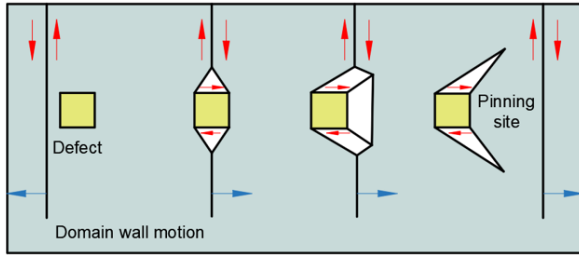


Figure 4. Movement of domain walls.

The MBN experimental setup consists of a signal generator, two amplifiers, a U-shaped core (ferrite yoke), a coil to capture the magnetic flux change (MBN sensor), and a data processing card/oscilloscope (Figure 5). The signal generator is used for getting alternating magnetic fields. Both sinusoidal (Ping et al., 2013; Ghanei et al., 2014) and triangular (Blaow et al., 2004; Hucailuk et al., 2015) waveforms have been used in research. The frequency interval applied to get the magnetic field divides into two parts high frequency (>10 Hz) and low

frequency (<1 Hz). High frequencies cause low measurement depths (Lo et al., 2000; Moorthy et al., 2005; Wilson et al., 2009). Ferrite yoke and MBN sensors are placed on the sample. Ferrite yoke is shaped U and made with Fe-Si alloy to increase the effect of the magnetic field. It can also be produced in different shapes according to the surface on which the measurement is done. The sinusoidal/ triangular wave produced by the signal generator is oriented with the yoke to create the magnetic field. The MBN sensor senses the magnetic flux changes, filtered by boosting with the amplifier. The signals are transferred to the computer using a data processing card or oscilloscope. A typical BN signal obtained by a magnetism circuit is seen in Figure 6. MBN events during the current have small amplitude. Therefore, a much smaller signal is generated on the magnetic hysteresis. This makes it necessary to filter the MBN signal. Filtering is done with a high-pass or band-pass filter in signal processing electronics (Figure 7.a). Typical band-pass filtering can be from 300 Hz to 300 kHz. Alternatively, a ferromagnetic core and a receiver coil are placed vertically on the test specimen. During magnetization, the small magnetic core will be magnetically connected to the core (Figure 7.b). Thus, the small magnetic core will not be affected by voltage induction. Magnetic core should be made of a material which has much lower MBN activity than the main sample (Zurek, 2017).

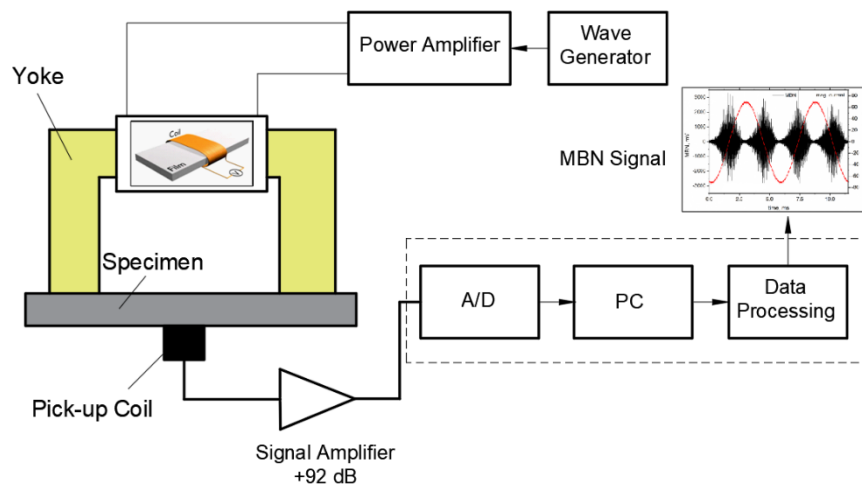


Figure 5. MBN experimental setup.

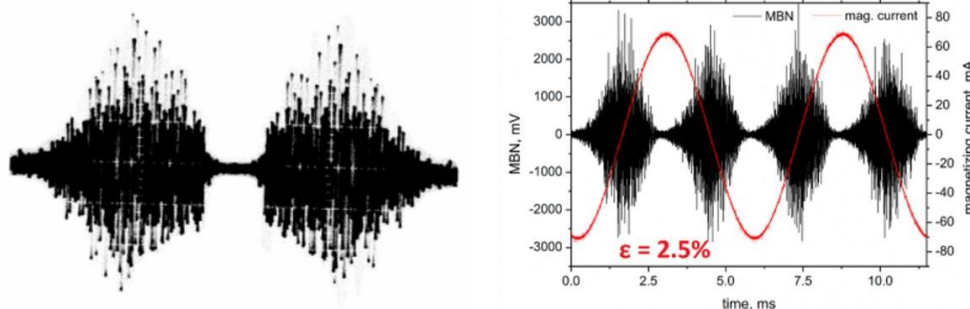


Figure 6. BN signal.

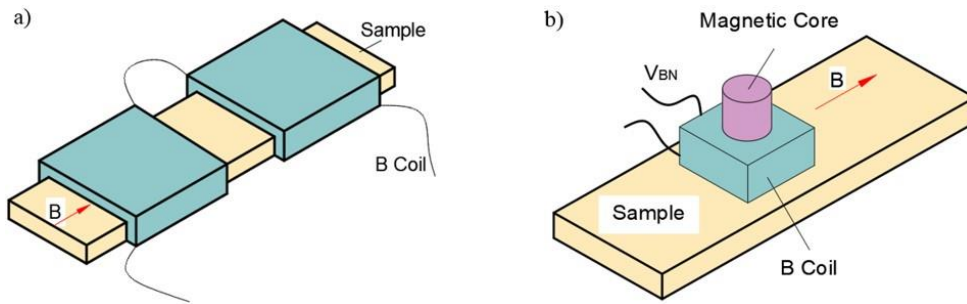


Figure 7. a) Using band-pass filter b) Using magnetic core.

### 2.2. MBN Signal

As obtained signals are produced as voltage impulses by MBN sensor, they require statistical analysis. A signal obtained with a magnetic circuit consists of two parts. One represents the circuit's positive side, and the other represents the negative side. The average of them is nominally zero (Blaow et al., 2006). Thus, parameters need to explain both the positive and the negative amplitudes of sudden BN incidents (Iordache et al., 2003).

To compare it with previous works, researchers generally use different methods of BN signal analysis. The most common ones of them are the number of the total peak, Total Sum of Amplitudes (TSA), and Root Mean Square (RMS) (Figure 8).

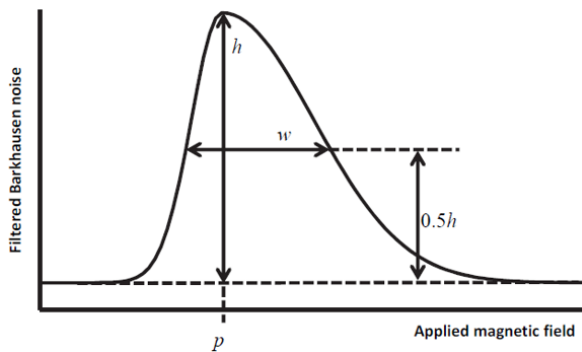


Figure 8. Calculation of peak width.

Data of BN obtained during a magnetization circuit hide in a sequence. The sequence's total amplitude of absolute values is added together in 20 consecutive cycles. To represent the BN events better (equation 1):

$$\text{Sum of Amplitudes} = \sum_{n=1}^{z=20} (\sum_{k=1}^m (|a_k|))_n \quad (1)$$

RMS (equation 2) is the most used parameter of BN and easy to calculate (Spaldin, 2010). where N = number of elements in the input sequence and Xi is the MBN amplitudes.

$$\text{RMS} = \sqrt{\frac{1}{N} \sum_{n=1}^N x_i^2} \quad (2)$$

Another essential feature of MBN energy is derived using the squared signal and one MBN envelope. The two features are integrated into each other (Kim et al. 1992). The envelope consists of measurements from half of one

magnetization loop. Then, BN energy is calculated from all measurement signals (Gauthier et al., 1998). Peak position (p) and height (h) are obtained by fitting a second-order polynomial to the profile top. Figure 8 shows peak height (h) and peak weight (w). Peak width (w) can be calculated using different peak heights (0.25, 0.5 and 0.75) (Sorsa and Leiviskä, 2009).

### 3. The Relationship between Material Characterization and MBN

The microstructure of the material affects magnetic characteristics of the materials. Many researchers have analyzed the relationship between the BN profile and microstructural properties of the material such as grain size, residual stress, grain segregation (Ranjan et al., 1987; Moorthy et al., 1997; Anglada-Rivera et al., 2001; Yamaura et al., 2001; Kim and Kwon, 2003), phase structure (Saquet et al., 1999; Moorthy et al., 2000; D'Amato et al., 2003; Koo et al., 2003; Kaplan et al., 2007; Kleber et al., 2008), or carbon content (Gatelier-Rothea et al., 1998; Koo et al., 2003; Capó-Sánchez et al., 2004; Pérez-Benitez et al., 2005) in the internal structure.

The number of magnetic domains and domain walls increases with the decrease of grain size in microstructure. The increase in the number of the domain walls leads to more magnetic flux bounces but smaller amplitudes (Anglada-Rivera et al., 2001; Sipahi, 1994). Furthermore, it is determined that increasing carbon content also makes the particle size smaller, so it raises the activities of MBN (Capó-Sánchez et al., 2004; D'Amato et al., 2003). It's established that there is a good correlation between the MBN profile and the ferrite amount ( Moorthy et al., 2000; Kleber et al., 2008) of the material together with the contents of martensite (Saquet et al., 1999) and pearlite (Koo et al., 2003).

Because of the increase in the hardness of the material, the movements of the domain walls get complicated, and so it causes a decrease in MBN activity (Sipahi, 1994; Cullity and Graham, 2011). With the increasing hardness, the value of Magnetic Barkhausen Noise RMS and peak altitude are determined to decrease.

MBN is too sensitive for the stress situations on the material (Stefanita et al., 2000b). Truong it can use the assessments of stress situations. It has been found that BN activity increases during tensile stress, while it

decreases during compressive stress (Jagdish et al., 1990; Lindgren and Lepistö, 2002; Santa-aho et al., 2009). The changes in the stress situation can be found by using the characteristics of the BN profile like its RMS value, peak altitude, BN energy, and peak position/amplitude (Gatlier-Rothea et al., 1998; Gauthier et al., 1998; Lindgren and Lepistö, 2002; Iordache et al., 2003; Blaow et al., 2007;). The measuring device should be calibrated for each material while measuring stresses (Gauthier et al., 1998; Lindgren and Lepistö, 2002; Blaow et al., 2007). This is because many factors affect the BN in the internal structure of the material. These make the estimation of residual stress more difficult. It is also reported that measuring direction affects the measurement and should be taken into consideration with the application of MBN noise measurement (Ruikun et al., 2021).

#### 4. Applications of MBN

##### 4.1. Deformation state detection

Materials under stress deform and change shape or fracture/failure may occur. The amount of deformation that occurs because of stress varies according to the material. The change in the shape of material is experienced in two ways: elastic and plastic. Plastic deformation comprises four phases: perfectly elastic, micro-yielding, macro-yielding, and progressive plastic deformation (Moorthy et al., 1999). The deformation starts at stresses lower than the yield strength.

MBN is preferred for NDT determination of elastic and plastic deformation of materials because it has a high sensitivity to stress (Moorthy et al., 1999; Stefanita et al., 2000a; Dhar et al., 2001; Kleber and Vincent, 2004). MBN can be used in different deformation stages ( Moorthy et al., 1999; Iordache et al., 2003). One of the advantages of MBN compared with other methods is that different stages of deformation can be determined and differentiated according to the obtained results (Moorthy et al., 1999; Iordache et al., 2003). Accordingly, BN can be used for situation assessment of parts and structures within their service lives. According to the deformation situation, the changes that took place in MBN are shown in Table 1.

Piotrowski (Piotrowski et al., 2009) examined magnetic hysteresis loops B(H), magnetic Barkhausen noise (MBN) and magnetoacoustic emission (MAE) signals in Fe-2%Si samples with up to 8% plastic deformation. They stated that the hysteresis loops properties and the MBN signal intensity changed rapidly from the first stages of plastic deformation. They showed that the MBN signal is very sensitive to the initial stage of deformation and can be used to determine the onset of deformation. In addition, there are studies examining changes in MBN signal below yield point changes in MBN signal in plastic deformation (Stefanita et al., 2000b) and changes caused by cold rolling (Stefanita et al., 2001).

**Table 1.** Deformation and Bn

Kind of Deformation	Feature of BN	Increase/Decrease
Tensile Elastic Strain	MBN energy and peak height	Increase ( Kleber and Vincent, 2004; Ruikung et al., 2021)
Compressive stress	MBN energy and peak height	Decrease (Moorthy et al., 1999)
Initiation of micro yielding	MBN Amplitude	Decrease (Kleber and Vincent, 2004; Piotrowski et al., 2009; Hucauluk et al., 2015)
Early stage of plastic deformation	MBN activity	Increased ( Moorthy et al., 1999; Stefanita et al., 2000a; Kleber and Vincent, 2004)
Final stage of plastic deformation	MBN activity	Decrease (Moorthy et al., 1999)
Rolling direction	MBN activity	Increased (Stefanita et al., 2001; Schijve, 2009)

##### 4.2. Fatigue Monitoring

Fatigue essentially describes changes in a material which the initiation and propagation of cracks when it is under a cyclic load. The mechanism of fatigue has three steps. Once: a small amount changes leading to crack initiation, crack growth, and lastly: the fracture of the material (Sagar et al., 2005; Schijve, 2009). The BN method is an alternative method for fatigue monitoring (Vincent et al., 2005). A typical nonlinear relationship is detected between BN and the number of stress cycles (Błachnio et al., 2002) because fatigue at different stages affects BN differently (Table 2). This situation has been confirmed by the microstructure changes caused by dislocation movements (Govindaraju et al., 1993; Lindgren and Lepistö 2003; Sagar et al., 2005).

##### 4.3. Case Depth Evaluation

BN is susceptible to alteration in the surface condition of ferromagnetic material. The frequency bandwidth of the BN signal can be used to analyze the material condition at different depths. Steel's frequency range is between 20-160 kHz. Changes in the material at different depths are evaluated according to the change in the high-frequency components of the BN signal. Jiles and Suominen (Jiles and Suominen, 1994) showed the relationship between BN and the stress on the material surface. Accordingly, the BN envelope signal gradually decreased with the compressive stress. In the study, 5 different frequency values were used to determine the depth of penetration of the BN signal to the surface. In Table 3, the frequency value and the corresponding depth of penetration are given.

**Table 2.** Fatigue and MBN

Kind of fatigue	Feature of MBN	Increase/ Decrease
First stage	MBN activity	Increase
Second stage	MBN activity	Decrease
Final stage	MBN activity	Further increase

**Table 3.** Penetration depth of MBN at different detection frequency bandwidths

Bandwidths (kHz)	Penetration Depth (mm)
120-160	$95 \times 10^{-3}$
100-120	$107 \times 10^{-3}$
80-100	$119 \times 10^{-3}$
50-80	$140 \times 10^{-3}$
20-50	$190 \times 10^{-4}$

#### 4.4. Grinding Burn Detection

The grinding process is used for the surface finishing of a component/product. But during this process, undesirable conditions may occur on the part's surface. These undesirable situations may be softening or burns, residual stress, and micro-cracking. The reason for this is the increased localized temperatures (Malkin and Guo, 2008). Some studies on BN have shown that grinding burns on the surface can be detected by using the BN method. The peak height (h) and width (w) are sensitive to grinding burns (Gupta et al., 1997; Wilson et al., 2009). Moorthy et. al detected grinding burns using low and high-frequency values (Moorthy et al., 2005). As a result, they obtained a single peak BN profile at high-frequency measurements and a two peak BN profile at low frequencies. They stated that the peak height of the high-frequency profile accorded well with the residual stress changes due to grinding damage. The second peak of the low-frequency profile was indicated to echo the changes in stresses and microstructure near the surface. It is also known to be widely used by the US air force and navy department, SAE, FAA and AST. On the other hand, it is known that this method has been used successfully in the evaluation of coating thicknesses on aircraft landing gear (Jiles et al., 1989).

#### 4.5. Corrosion and surface treatments evaluation

In the modern world, the importance of steel, which is used in many fields from the automotive industry to many machine parts, from the ship industry to the construction industry and steel constructions, increases day by day. Steels are widely used because they are relatively inexpensive, have high strength and hardness, are suitable for manufacturing methods such as welding and casting, and are relatively easy to process. Although steels have specified properties, they have some disadvantages. The most important of these disadvantages is corrosion. The weakening of the material occurs with the narrowing of the cross-section of the steels as a result of the surface oxides formed

especially in the ship and machine parts, vehicles or steel construction structures operating in marine atmospheres (Antunes et al., 2014; Pastorek et al., 2021). Today, material losses caused by steel structures and machine parts damaged because of corrosion constitute an important part of the country's economy. In addition to the direct economic losses that occur as a result of corrosion, the cost of damage increases significantly as a result of indirect losses such as production stoppage, energy losses, accidents, environmental effects and loss of time (Secer and Uzun, 2017). On the other hand, various measures are taken to reduce corrosion damage. Despite these precautions, it is not possible to prevent corrosion damage. The most effective method to minimize the effects of corrosion is the early-stage detection of corrosion. For this reason, it is important that corrosion damage can be detected beforehand (Agarwala et al., 2000; Liu et al., 2022; Zhang and Tian, 2016).

There are various industrially used methods such as ultrasonic method (Zhang et al., 2021), ultrasonic tomography (Martin et al. 2001), gamma rays (Peng and Wang, 2015), magnetics flux leaking method (Christen et al., 2009) for the evaluation of corrosion to which a steel machine part or construction is exposed. On the other hand, another method that can be an alternative to these methods is the BN method (Neslušan et al., 2019; Pastorek et al., 2021).

As a result of corrosion, a new oxide layer is deposited on the surface of the material or material dissolutions such as microcracks may occur (Tullmin and Roberge, 1995). Corrosion causes various changes in the internal structure and surface properties of the material (Manh et al., 2020). For example, in Figure 9, a cross-sectional view of a steel piece exposed to oxidation for 24 hours at 625 °C in open atmosphere conditions and Figure 10, SEM image of the metallic layer formed/deposited on the surface of the corroded steel wire is given.

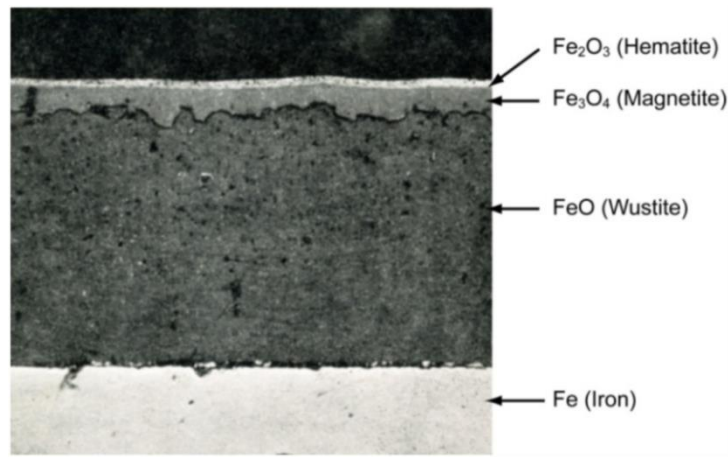


**Figure 9.** Cross-section of oxide layers formed on iron in air at 625 °C after 24 hours (Mrowec, 1967; Colwell and Babic, 2012).

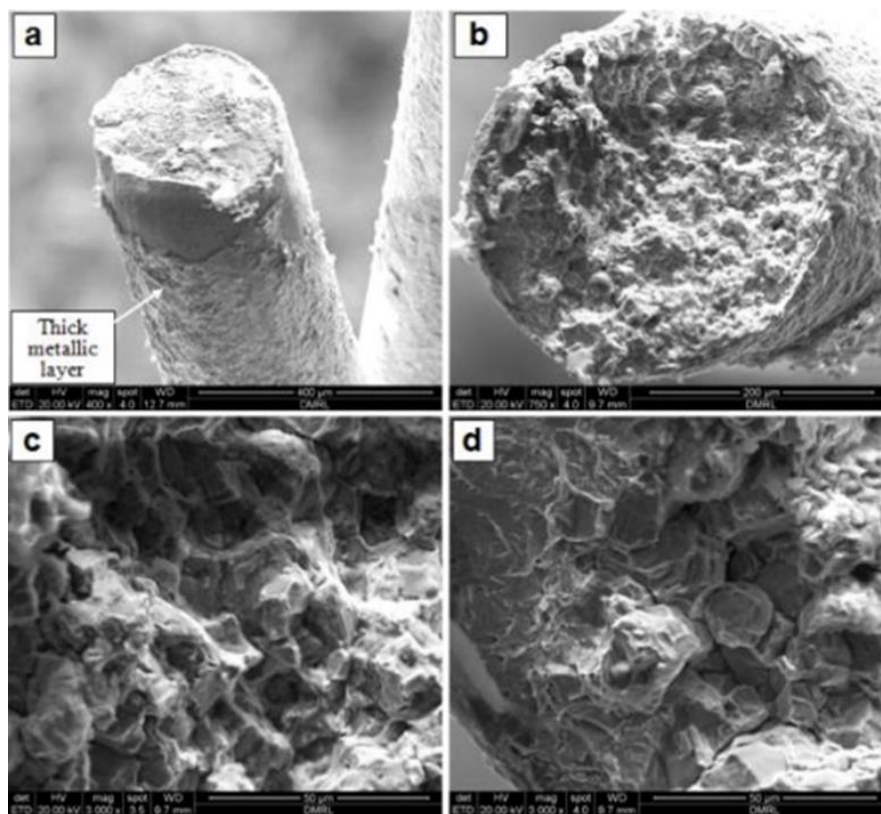


**Figure 10.** SEM image of steel wire (Li et al., 2017; Rao and Singh, 2019).

Steel materials are affected by acids and gases such as HCl, HCL, SO<sub>2</sub> SO<sub>3</sub>, NO, NO<sub>2</sub>, H<sub>2</sub>SO<sub>4</sub> and NH<sub>3</sub> in their environment and suffer corrosion damage (Colwell and Babic, 2012; Leygraf et al., 2016; So et al., 2020). Such corrosive environments also change the structure of the surface and near-surface areas. As it is known, the BN technique is very sensitive to microstructural changes such as mechanical stresses, chemical composition and grain size, inclusions, precipitates, and dislocations (Tuzun et al., 2023). This situation causes changes in the BN envelope with the section exposed to corrosion. For this reason, the BN method is used as an alternative method for the detection of corrosion damage. Various studies on the MBN method have shown that corrosion

damage can be successfully evaluated. (Neslušan et al., 2019) investigated the detectability of corrosion damage in steel wire rope using the BN Method. At the end of the study, it was reported that using BN Method, corrosion can be detected, and the thickness of the steel rope wire can be determined. Pastorek et al. (2021) used different low alloy steel materials with yield strengths of 235, 700, and 1100 MPa. The prepared samples were subjected to various levels of corrosion using the STN EN ISO 9227 standard in the VSC KWT 1000 chamber. The temperature was maintained at 35°C, with a pH range of 6.5 to 7.2, and a chamber pressure of 120 kPa. It was observed that MBN activities decreased as the worn layer thickness on the sample increased (as the base metal

thickness decreased). Especially in the early stages of corrosion (low number of days in the chamber), MBN activities decrease steeply and then reach saturation. This is because it inhibits MBN activities by increasing the corroded layer thickness. (Jančula et al., 2021) have reached similar findings in their study on Steel S460MC

to examine the relationship between MBN and corrosion. Figure 11.a shows that as the corrosion time increases, the corroded layer thickness increases, and the wall thickness decreases. Figure 11.b shows the relationship between corrosion exposure time and MBN activity.

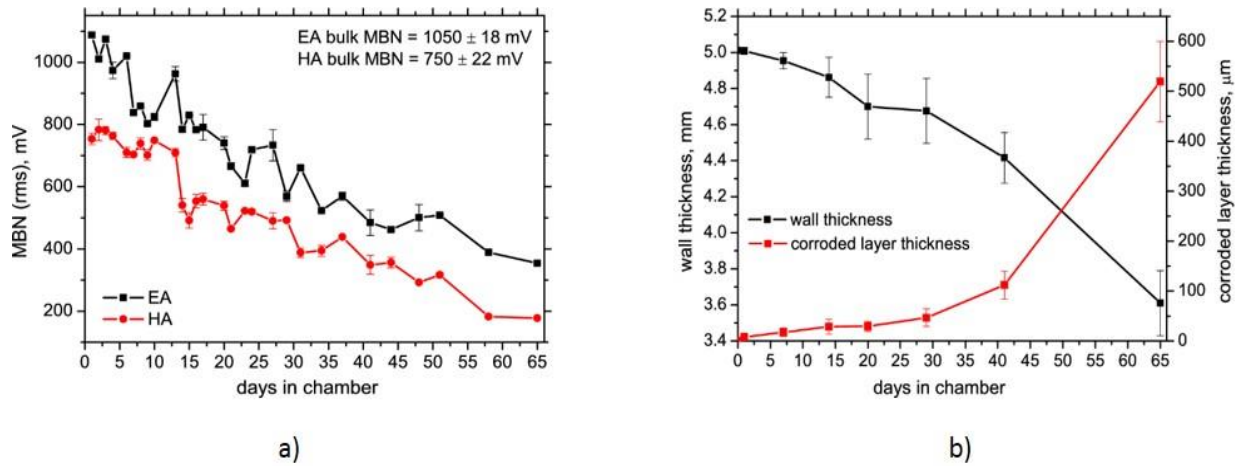


**Figure 11.** Relationship between MBN and corrosion (Jančula et al., 2021), a) Wall and corroded layer thickness, b) MBN and days in the chamber.

#### 4.6. Surface treatments evaluation

All the wear, corrosion, etc. damage that the materials are exposed to depending on the environment in service conditions begin on the surfaces of the material facing the atmosphere or the service environment. For this reason, the use of a coating suitable for the surface properties of a material is effective in reducing damages such as wear and corrosion that may occur in the material (Kocaman et al., 2020). On the other hand, no coating method is sufficient to preserve a material forever. For this reason, the service life of a coated material affects the coating performance depending on many parameters such as the thickness of the coating applied to the material and the phases formed on the surface. For this reason, both determining the performance of a coated material and using the material with the highest efficiency and time in the environment to which the material is exposed under service conditions depends on the examination of the uncoated material and periodic maintenance. The use of non-destructive testing method in periodical maintenance and inspection of materials under service conditions is a fast and economical method. In the literature, non-destructive testing methods such as ultrasonic method (Honarvar and Varvani-Farahani 2020), laser ultrasonic, infrared thermography, X-ray radiography, eddy current (Alamin et al., 2012; Kittinan et al., 2019) and acoustic emission (Tian-Shun et al., 2019) can be used in the control of coated samples and examining various properties such as coating thickness. Among these methods, the relatively newly developed BN method is an alternative to other non-destructive testing methods in the evaluation of coated materials (Jayakumar et al. 2012; Rao and Jayakumar, 2012). Krkoška et al. (2020) used BN method

for the evaluation of parts exposed to different surface treatments such as galvanization, phosphorization and compaction. BN signals are associated with metallographic and SEM observations as well as microhardness measurements. Figure 12 shows the SEM image of the crack under the wire coating to which the BN signal responds. Neslušán et al. (2017) investigated the thickness of the heat-affected zone, dislocation density, microhardness profile, and carbide distribution in 18NiCrMo14-6 material. These characteristics were examined after surface hardening using the MBN method. Santa-aho et al. (2012) performed the hardening process on 34CrNiMo6 and 42CrMo4 steels. As a result, they used the BN method to evaluate the hardening depth and found that the results were consistent with the destructive testing of the cross-section of the specimen (Santa-aho et al., 2012). Stupakov et al changed the surface carbon concentration by decarburizing EN 54SiCr6 steel material in their study (Stupakov et al., 2011). As a result of the study, they determined the depth of decarburization in the material with MBN and suggested that the method can be used in practical applications with certain parameters (Figure 13 a-b). Sorsa et al. (2019) used the BN method to measure the nitriding thickness of 32CrMoV5 (GKP), BS S132 (S132), 709M40 (En19), and 722M24 (En40B) steels in which they applied nitriding process. At the end of the study, the researchers stated that the BN method could be used efficiently in the evaluation of the nitride layer. Čilliková et al., (2020) evaluated the thermal damage of the material after quenching of 100Cr6 steel using the MBN Method and its effects on the hardness of the coating process. Seemuang and Slatter (2017) coated high speed tool steel with EBPA-PVD method using two different



coating materials (TiN or CrN) and 3 different coating thicknesses (~5, 10.9 and 14.4 micron). They used the BN method to measure the coating depths on the high-speed tool steel they covered. As a result of the study, they reported that the BN method can be used

successfully in the evaluation of coating thicknesses. (Saquet et al., 1998) measured the depth of hardening after nitriding on steel using the BN Method. Successful results were obtained at the end of the study.

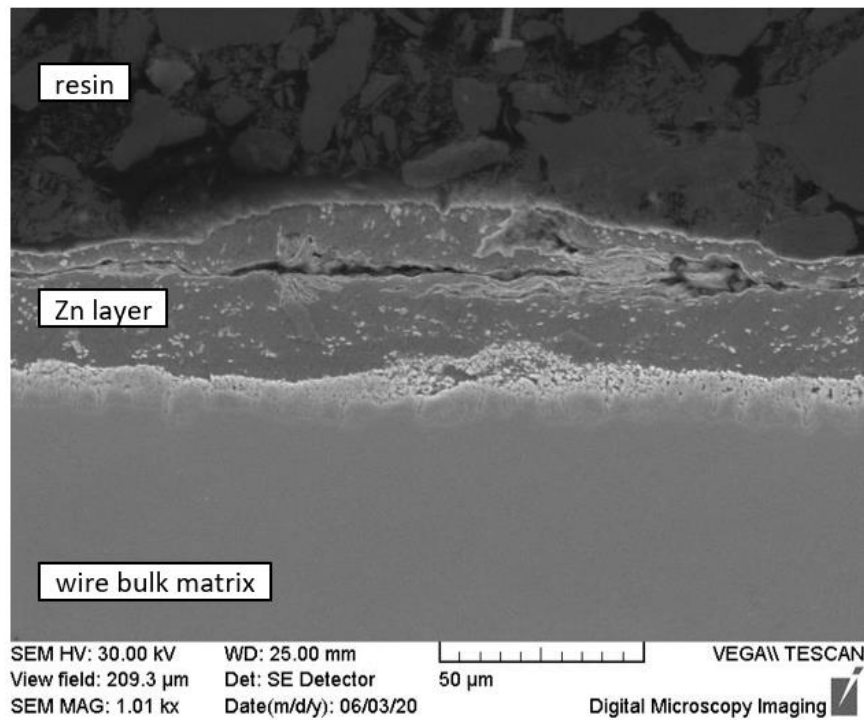


Figure 12. Galvanized steel wire section view (Krkoška et al., 2020).

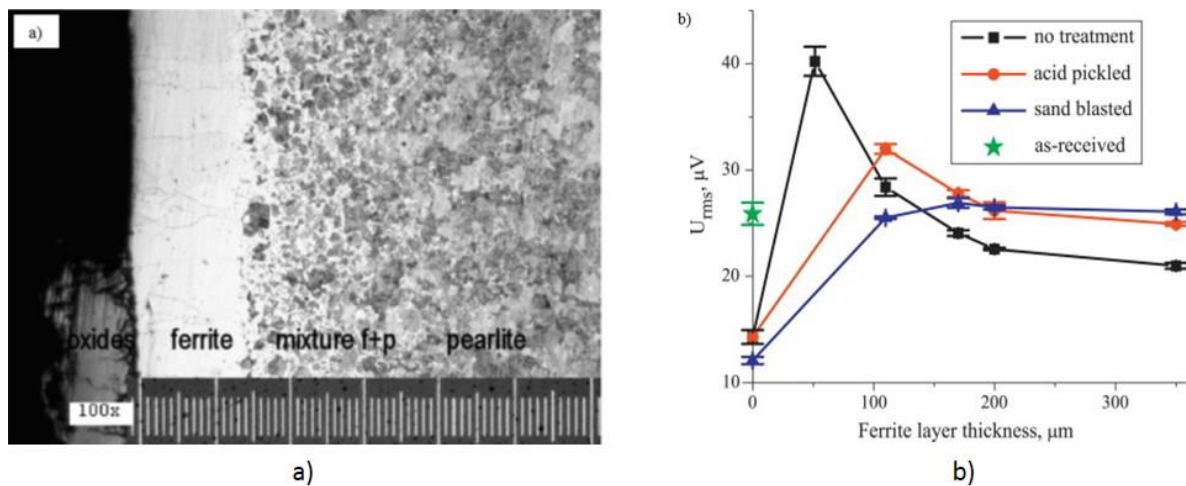


Figure 13. a) After the decarburization process, metallographic picture of cross-section of the sample (Stupakov et al., 2011) and b) Dependence of the rms value of BN voltage.

### 5. Results

In this paper, MBN, which is one of the non-destructive testing methods, is discussed. Basic concepts of the MBN method like domain, domain walls, dipole, and hysteresis loop have been explained. Necessary equipment for the measurements has been defined. With the literature review, it is determined that the BN profile is sensitive to the microstructure of the material, its grain size, hardness, phase structure, stress, and residual stress. It is seen that it can be used for many NDT experiments. MBN

method has a wide area of application, such as product quality control and product improvement, strength estimation, determination of deformation/fatigue situation, and examination of the surface situation. This method stands out mainly due to the affordable equipment prices, its compliance with automation, and applicability during the manufacture/service period.

**Author Contributions**

The percentage of the author(s) contributions is presented below. All authors reviewed and approved the final version of the manuscript.

	Ö.A.	O.K.	A.S.G.	E.K.	E.B.
C	10	40	10	20	20
D	10	10	30	25	25
S	25	25	20	20	10
DCP	25	25	10	20	20
L	20	20	20	20	20
W	20	20	20	20	20
CR	20	20	20	20	20
SR	20	20	20	20	20

C= concept, D= design, S= supervision, DCP= data collection and/or processing, L= literature search, W= writing, CR= critical review, SR= submission and revision.

**Conflict of Interest**

The authors declare that there is no conflict of interest.

**References**

Agarwala VS, Reed PL, Ahmad S. 2000. Corrosion detection and monitoring - a review. *Corrosion* 2000, March26-31, Orlando, Florida, USA, pp: 272.

Alamin M, Tian GY, Andrews A, Jackson P. 2012. Principal component analysis of pulsed eddy current response from corrosion in mild steel. *IEEE Sens J*, 12(8): 2548-53.

Anglada-Rivera J, Padovese LR, Capó-Sánchez J. 2001. Magnetic barkhausen noise and hysteresis loop in commercial carbon steel: influence of applied tensile stress and grain size. *J Magn Mater*, 231(2): 299-306.

Antunes RA, Ichikawa RU, Martinez LG, Costa I. 2014. Characterization of corrosion products on carbon steel exposed to natural weathering and to accelerated corrosion tests. *J Bio Tribocorros*, 2014: e419570.

Blachnio J, Dutkiewicz J, Salamon A. 2002. The effect of cyclic deformation in a 13% cr ferritic steel on structure and barkhausen noise level. *Mater Sci Eng A Struct Mater*, 323(1): 83-90.

Blaow M, Evans JT, Shaw B. 2004. Effect of deformation in bending on magnetic barkhausen noise in low alloy steel. *Mater Sci Eng A Struct Mater*, 386(1): 74-80.

Blaow M, Evans JT, Shaw BA. 2007. The effect of microstructure and applied stress on magnetic barkhausen emission in induction hardened steel. *J Mat Sci*, 42(12): 4364-71.

Blaow, M, Evans JT, Shaw BA. 2006. Effect of hardness and composition gradients on barkhausen emission in case hardened steel. *J Magn Mater*, 303(1): 153-59.

Blitz J. 2012. *Electrical and magnetic methods of non-destructive testing*. Springer Science & Business Media, London, UK, pp: 125.

Capó-Sánchez J, Pérez-Benitez J A, Padovese L R, Serna-Giraldo C. 2004. Dependence of the magnetic barkhausen emission with carbon content in commercial steels. *J Mater Sci*, 39(4): 1367-70.

Christen R, Bergamini A, Motavalli M. 2009. Influence of steel wrapping on magneto-inductive testing of the main cables of suspension bridges. *NDT E Int*, 42(1): 22-27.

Chung T, Lee JR. 2018. Thickness reconstruction of nuclear power plant pipes with flow-accelerated corrosion damage

using laser ultrasonic wavenumber imaging. *Struct Health Monit*, 17(2): 255-65.

Čilliková M, Uriček J, Neslušán M, Ballo V, Mičietová A. 2020. Monitoring of thermal damage after deposition of coatings via barkhausen noise technique. *Acta Phys Pol A*, 137(5): 637-39.

Clapham, L, White S, Lee J, Atherton DL. 2000. Magnetic easy axis development in steel—the influence of manufacturing. *J Appl Phys*, 88(4): 2163-65.

Colwell JD, Babic D. 2012. A review of oxidation on steel surfaces in the context of fire investigations. *SAE Inter J Cars - Mechan Syst*, 5(2): 1002-15.

Cullity BD, Graham CD. 2011. *Introduction to magnetic materials*. John Wiley & Sons, London, UK, pp: 54.

D'Amato C, Verdu C, Kleber X, Regheere G, Vincent A. 2003. Characterization of austempered ductile iron through barkhausen noise measurements. *J Nondestr Eval*, 22(4): 127-39.

Dhar A, Clapham L, Atherton DL. 2001. Influence of uniaxial plastic deformation on magnetic barkhausen noise in steel. *NDT E Int*, 34(8): 507-14.

Durin G, Zapperi S. 2004. The barkhausen effect. *Sci Hyster*, 2004: 181-267.

Fischer P. 2013. Imaging magnetic structures with polarized soft x-rays. *Synchrot Radiat News*, 26(6): 12-19.

Gatelier-Rothea C, Chicois J, Fougères R, Fleischmann P. 1998. Characterization of pure iron and (130p.p.m.) carbon-iron binary alloy by barkhausen noise measurements: study of the influence of stress and microstructure. *Acta Materialia*, 46(14): 4873-82.

Gauthier J, Krause T W, Atherton DL. 1998. Measurement of residual stress in steel using the magnetic barkhausen noise technique. *NDT E Int*, 31(1): 23-31.

Ghanei S, Alam AS, Kashefi M, Mazinani M. 2014. Nondestructive characterization of microstructure and mechanical properties of intercritically annealed dual-phase steel by magnetic barkhausen noise technique. *Mater Sci Eng A Struct Mater*, 607:253-60.

Govindaraju MR, Strom A, Jiles DC, Biner SB, Chen ZJ. 1993. Evaluation of fatigue damage in steel structural components by magnetoelastic barkhausen signal analysis. *Appl Phys Lett*, 73(10): 6165-67.

Graham DC, Chikazumi S. 1997. *Physics of ferromagnetism*. Calenderon Press, New York, USA. pp: 211-328.

Gupta H, Zhang M, Parakka AP. 1997. Barkhausen effect in ground steels. *Acta Material*, 45(5): 1917-21.

Honarvar F, Varvani-Farahani A. 2020. A review of ultrasonic testing applications in additive manufacturing: defect evaluation, material characterization, process control. *Ultrasonics*, 108: 106227.

Hucailuk C, Nuñez N, Torres D. 2015. Study by magnetic barkhausen noise of a 1020 steel and 99.9% nickel plate. *Proced Mat Sci*, 9: 313-18.

Iordache VE, Hug E, Buiron N. 2003. Magnetic behavior versus tensile deformation mechanisms in a non-oriented fe-(3 wt.%)si steel. *Mater Sci Eng A Struct Mater*, 359(1): 62-74.

Jagadish C, Clapham L, Atherton DL. 1990. Influence of uniaxial elastic stress on power spectrum and pulse height distribution of surface barkhausen noise in pipeline steel. *IEEE Trans Magn*, 26(3): 1160-63.

Jančula M, Neslušán M, Pastorek F, Pitoňák M, Pata V, Minárik P, Gocál J. 2021. Monitoring of corrosion extent in steel s460mc by the use of magnetic barkhausen noise emission. *J Nondestr Eval*, 40(3): 69.

Jayakumar T, Rao BPC, Mukhopadhyay CK, Viswanath A,

- Vaidyanathan S. 2012. Advances in electromagnetic non-destructive techniques for characterization of metallic materials. *Electromagnetic Nondestructive Evaluation*, IOS Press, India, New Delhi, 36<sup>th</sup> ed., pp: 79-86.
- Jiles D, Suominen L. 1994. Effects of surface stress on barkhausen effect emissions: model predictions and comparison with x-ray diffraction studies. *IEEE Trans Magn*, 30(6): 4924-4926.
- Jiles DC, Garikipati P, Palmer DD. 1989. Evaluation of residual stress in 300m steels using magnetization, barkhausen effect and x-ray diffraction techniques. In: Thompson DO and Chimenti DE, editors. *Review of Progress in Quantitative Nondestructive Evaluation*. Boston, USA, 8th ed., Part A and Part B, pp: 2081-2087.
- Kaplan M, Gür CH, Erdogan M. 2007. Characterization of dual-phase steels using magnetic barkhausen noise technique. *J Nondestr Eval*, 26(2): 79-87.
- Kemal D, Gür CH. 2008. Manyetik barkhausen gürültüsü yöntemi ile çeliklerde tahribatsız içyapı karakterizasyonu. 3<sup>rd</sup> International Non-Destructive Testing Symposium and Exhibition, 17-19 April, Istanbul, Türkiye, pp: 243.
- Kim DW, Kwon D. 2003. Quantification of the barkhausen noise method for the evaluation of time-dependent degradation. *J Magn Mater*, 257(2): 175-83.
- Kim HC, Lee HK, Kim C G, Hwang DG. 1992. Barkhausen noise in ferromagnetic metallic glass Fe<sub>40</sub>Ni<sub>38</sub>Mo<sub>4</sub>B<sub>18</sub>. *Appl Phys Lett*, 72(8): 3626-33.
- Kittinan S, Noipitak M, Sae-Tang W. 2019. Detection of corrosion under coated surface by eddy current testing method. 7<sup>th</sup> International Electrical Engineering Congress (IEECON), Hua Hin, Thailand, pp: 1-4.
- Kleber X, Hug-Amalric A, Merlin J. 2008. Evaluation of the proportion of phases and mechanical strength of two-phase steels using barkhausen noise measurements: application to commercial dual-phase steel. *Metall Mater Trans A Phys Metall Mater Sci*, 39(6): 1308-18.
- Kleber X, Vincent A. 2004. On the role of residual internal stresses and dislocations on barkhausen noise in plastically deformed steel. *NDT E Int*, 37(6): 439-445.
- Kocaman E, Kiliç B, Şen Ş, Şen U. 2020. Krom içeriğinin Fe(18-x)Cr<sub>x</sub>B<sub>2</sub> (X=3,4,5) sert dolgu elektrotunda mikroyapı, aşınma ve korozyon davranışı üzerindeki etkisi. *Gazi Üniv Müh Mimar Fak Derg*, 36(1): 177-90.
- Koo K M, Yau M Y, Dickon H L, Ng, C. C. H. Lo. 2003. Characterization of pearlite grains in plain carbon steel by barkhausen emission. *Mater Sci Eng A Struct Mater*, 351(1): 310-15.
- Krkoška L, Moravčík M, Zgútová K, Neslušán M, Uhřík M, Bahleda F, Pitoňák M. 2020. Investigation of barkhausen noise emission in steel wires subjected to different surface treatments. *Coatings*, 10(10): 912.
- Le TM, Benitez JAP, Hernandez JHE, Hallen JM. 2020. Barkhausen noise for non-destructive testing and materials characterization in low carbon steels. In: Manh TL, Benitez JAP, Hernández JHE, López JMH editors. *Woodhead Publishing Series in Electronic and Optical Materials*. Woodhead Publishing, Sawston, UK, pp: 115-146.
- Leygraf C, Graedel T, Tidblad J, Wallinder IO, Graedel T. 2016. *Atmospheric corrosion*. Wiley Interscience, New York, USA, 2<sup>nd</sup> ed., pp: 6-248.
- Li S, Hu P, Zhao X, Chen K, Li J. 2017. Atmospheric corrosion performance of wire rope sling in a sulfur dioxide-polluted environment. *Adv Mech Engin*, 9(6): 1-12.
- Lindgren M, Lepistö T. 2002. Application of barkhausen noise to biaxial residual stress measurements in welded steel tubes. *Mat Sci Technol*, 18(11): 1369-1376.
- Lindgren M, Lepistö T. 2003. Effect of cyclic deformation on barkhausen noise in a mild steel. *NDT E Int*, 36(6): 401-9.
- Liu H, Zhong J, Ding F, Meng X, Liu C, Cui J. 2022. Detection of early-stage rebar corrosion using a polarimetric ground penetrating radar system. *Constr Build Mater*, 317: 125768.
- Lo CCH, Tang F, Biner SB, Jiles DC. 2000. Effects of fatigue-induced changes in microstructure and stress on domain structure and magnetic properties of Fe-C alloys. *Appl Phys Lett*, 87(9): 6520-22.
- Malkin S, Guo C. 2008. *Grinding technology: theory and application of machining with abrasives*. Industrial Press Inc, New York, USA, pp: 231.
- Manh TL, Benitez JAP, Alberteris M. 2020. Barkhausen noise for nondestructive testing and materials characterization in low-carbon steels. In: Manh TU, Benitez JAP, Hernandez JHE, Lopez JMH, 9 - Future Trend and Applications of Barkhausen Noise, Woodhead Publishing Series in Electronic and Optical Materials, Woodhead Publishing, New York, USA, pp: 239-253
- Martin J, Broughton KJ, Giannopolous A, Hardy MSA, Forde MC. 2001. Ultrasonic tomography of grouted duct post-tensioned reinforced concrete bridge beams. *NDT E Int*, 34(2): 107-13.
- McMaster RC. 1959. *Nondestructive testing handbook*. Only edition, Ronald Phillips Ltd, New York, USA, pp: 141.
- Moorthy V, Shaw BA, Mountford P, Hopkins P. 2005. Magnetic barkhausen emission technique for evaluation of residual stress alteration by grinding in case-carburised en36 steel. *Acta Mater*, 53(19): 4997-5006.
- Moorthy V, Vaidyanathan S, Baldev R, Jayakumar T, Kashyap BP. 2000. Insight into the microstructural characterization of ferritic steels using micromagnetic parameters. *Metall Mater Trans A Phys Metall Mater Sci*, 31(4): 1053-1065.
- Moorthy V, Vaidyanathan S, Jayakumar T, Baldev R, Kashyap BP. 1999. Effect of tensile deformation on micromagnetic parameters in 0.2% carbon steel and 2.25Cr-1Mo steel. *Acta Mater*, 47(6): 1869-1878.
- Moorthy V, Vaidyanathan S, Jayakumar T, Baldev R. 1997. Microstructural characterization of quenched and tempered 0.2% carbon steel using magnetic barkhausen noise analysis. *J Magn Mater*, 171(1): 179-89.
- Mrowec, S. 1967. On the mechanism of high temperature oxidation of metals and alloys. *Corros Sci*, 7(9): 563-78.
- Neslušán M, Bahleda F, Minárik P, Zgútová K, Jambor M. 2019. Non-Destructive monitoring of corrosion extent in steel rope wires via barkhausen noise emission. *J Magn Mater*, 484: 179-187.
- Neslušán M, Čížek J, Kolařík K, Minárik P, Čilliková M, Melikhova O. 2017. Monitoring of grinding burn via barkhausen noise emission in case-hardened steel in large-bearing production. *J Mater Process Technol*, 240:104-17.
- Paper A, Willcox M, Mysak T. 2000. *An introduction to barkhausen noise and its applications*. Insight NDT, New York, USA, pp: 63.
- Pastorek F, Decký M, Neslušán M, Pitoňák M. 2021. Usage of barkhausen noise for assessment of corrosion damage on different low alloyed steels. *Appl Sci*, 11(22): 10646.
- Peng-Chi P, Wang CY. 2015. Use of gamma rays in the inspection of steel wire ropes in suspension bridges. *NDT E Int*, 75: 80-86.
- Pérez-Benitez JA, Capó-Sánchez J, Anglada-Rivera J, Padovese LR. 2005. A model for the influence of microstructural defects on magnetic barkhausen noise in plain steels. *J Magn Mater*, 288: 433-42.
- Ping W, Ji X, Yan X, Zhu L, Wang H, Tian G, Yao E. 2013. Investigation of temperature effect of stress detection based

- on barkhausen noise. *Sens Actuators A Phys*, 194: 232-239.
- Ping W, Zhu S, Tian GY, Wang H, Wilson J, Wang X. 2010. Stress measurement using magnetic barkhausen noise and metal magnetic memory testing. *Meas Sci Technol*, 21(5): 055703.
- Piotrowski L, Augustyniak B, Chmielewski M, Landgraf FJG, Sablik MJ. 2009. Impact of plastic deformation on magnetoacoustic properties of fe-2%si alloy. *NDT E Int*, 42(2): 92-96.
- Ranjan R, Jiles D, Rastogi P. 1987. magnetic properties of decarburized steels: an investigation of the effects of grain size and carbon content. *IEEE Trans Magn*, 23(3): 1869-76.
- Rao A, Singh A. 2019. Failure analysis of stainless steel lanyard wire rope. *J Appl Res Technol*, 16: 35-40.
- Rao BPC, Jayakumar T. 2012. Recent trends in electromagnetic nde techniques and future directions. 18<sup>th</sup> World Conference on Nondestructive Testing, 16-20 April, Durban, South Africa, pp: 1-11.
- Ruikun W, Zhang H, Yang R, Chen W, Chen G. 2021. Nondestructive testing for corrosion evaluation of metal under coating. *J Sensors* 2021: e6640406.
- Sagar S, Palit N, Parida S, Das G, Dobmann DK. Bhattacharya. 2005. Magnetic barkhausen emission to evaluate fatigue damage in a low carbon structural steel. *Int J Fatigue*, 27(3): 317-22.
- Santa-aho S, Vippola M, Lepistö T, Lindgren M. 2009. Characterization of case-hardened gear steel by multiparameter barkhausen noise measurements. *Insight - Non-Destructive Test Condit Monit*, 51(4): 212-16.
- Santa-aho S, Vippola M, Sorsa A, Leiviskä K, Lindgren M, Lepistö T. 2012. Utilization of barkhausen noise magnetizing sweeps for case-depth detection from hardened steel. *NDT E Int*, 52: 95-102.
- Saquet O, Chicois J, Vincent A. 1999. Barkhausen noise from plain carbon steels: analysis of the influence of microstructure. *Mater Sci Eng A Struct Mater*, 269(1): 73-82.
- Saquet, O, Tapuleasa D, Chicois J. 1998. Use of barkhausen noise for determination of surface hardened depth. *Nondestruct Test Eval*, 14(5): 277-292.
- Schijve J. 2009. *Fatigue of structures and materials*. Springer, Dordrecht, Netherlands, pp:5-9.
- Secer M, Uzun ET. 2017. corrosion damage analysis of steel frames considering lateral torsional buckling. *Procedia Eng*, 171: 1234-1241.
- Seemuang N, Slatter T. 2017. Using barkhausen noise to measure coating depth of coated high-speed steel. *Int J Adv Manuf Technol*, 92(1): 247-58.
- Sipahi LB. 1994. Effects of creep damage, shot peening, case hardening on magnetic barkhausen noise analysis. *IEEE Trans Magn*, 30(6): 4830-4832.
- So O, Ek O, Ri T. 2020. Corrosion evaluation on mild steel in different selected media. *Inter J Engin Appl Sci Technol*, 5(3): 33-38.
- Sorsa A, Leiviskä K. 2009. An entropy-based approach for the analysis of the barkhausen noise signal. *Proceedings of 7<sup>th</sup> International Conference on Barkhausen Noise and Micromagnetic Testing*, July 15-16, Aachen, Germany, pp: 85-96.
- Sorsa A, Santa-Aho S, Aylott C, Shaw BA, Vippola M, Leiviskä K. 2019. Case depth prediction of nitrided samples with barkhausen noise measurement. *Metals*, 9(3): 325.
- Spaldin NA. 2010. *Magnetic materials: fundamentals and applications*. Cambridge University Press, Cambridge, UK, 2<sup>nd</sup> ed., pp: 54.
- Stefanita CG, Atherton DL, Clapham L. 2000a. Plastic versus elastic deformation effects on magnetic barkhausen noise in steel. *Acta Mater*, 48(13): 3545-3551.
- Stefanita CG, Clapham L, Atherton DL. 2000b. Subtle changes in magnetic barkhausen noise before the macroscopic elastic limit. *J Mater Sci*, 35(11): 2675-2681.
- Stefanita CG, Clapham L, Yi JK, Atherton DL. 2001. Analysis of cold rolled steels of different reduction ratio using the magnetic barkhausen noise technique. *J Mater Sci*, 36(11): 2795-2799.
- Stupakov O, Perevertov O, Tomáš I, Skrbek B. 2011. Evaluation of surface decarburization depth by magnetic barkhausen noise technique. *J Magn Magn Mater*, 323(12): 1692-1697.
- Tian-Shun D, Ran W, Guo-Lu L, Ming L. 2019. Failure mechanism and acoustic emission signal characteristics of coatings under the condition of impact indentation. *High Temp Mat Proces*, 38(2019): 601-611.
- Tullmin M, Roberge PR. 1995. Corrosion of metallic materials. *IEEE Trans Reliab*, 44(2): 271-78.
- Tuzun, MY, Yalcin MA, Davut K, Kilicli V. 2023. Nondestructive microstructural characterization of austempered ductile iron. *Mat Test*, 65(3): 453-65.
- Vincent A, Pasco L, Morin M, Kleber X, Delnondedieu M. 2005. Magnetic barkhausen noise from strain-induced martensite during low cycle fatigue of 304l austenitic stainless steel. *Acta Mater*, 53(17): 4579-4591.
- Wilson JW, Tian GY, Moorthy V, Shaw BA. 2009. Magneto-Acoustic emission and magnetic barkhausen emission for case depth measurement in en36 gear steel. *IEEE Trans Magn*, 45(1): 177-83.
- Yamaura S, Furuya Y, Watanabe T. 2001. The effect of grain boundary microstructure on barkhausen noise in ferromagnetic. *Mater Acta Mater*, 49(15): 3019-27.
- Yasumitsu T, Hashimoto K, Osawa N. 1996. Nondestructive estimation of fatigue damage for steel by barkhausen noise analysis. *NDT E Int*, 29(5): 275-80.
- Yelbay HI. 2008. Tahribatsız yöntemlerle kalıntı gerilim ölçümündeki gelişmeler. 3<sup>rd</sup> International Non-Destructive Testing Symposium and Exhibition, April 17-19, İstanbul, Türkiye, pp: 1-9.
- Zhang J, Cho Y, Kim J, Malikov AKu, Kim YH, Yi JH, Li W. 2021. Non-destructive evaluation of coating thickness using water immersion ultrasonic testing. *Coatings*, 11(11): 1421.
- Zhang J, Tian GY. 2016. UHF RFID tag antenna-based sensing for corrosion detection & characterization using principal component analysis. *IEEE Trans Antennas Propag*, 64(10): 4405-14.
- Zurek S. 2017. *Characterisation of soft magnetic materials under rotational magnetisation*. Boca Raton: CRC Press, London, UK, 1<sup>st</sup> ed., pp: 51-268.